Comparative *Plasmodium* gene overexpression reveals distinct perturbation of sporozoite transmission by profilin

Yuko Sato[a,b,*], Marion Hliscs[a,c], Josefine Dunst[a,d], Christian Goosmann[e], Volker Brinkmann[e], Georgina N. Montagna[a,f], and Kai Matuschewski[a,g]

[a]Parasitology Unit and [e]Imaging Unit, Max Planck Institute for Infection Biology, 10117 Berlin, Germany; [b]Infectious Diseases Interdisciplinary Research Group, Singapore–Massachusetts Institute of Technology Alliance for Research and Technology, 138602 Singapore; [c]School of BioSciences, University of Melbourne, Parkville, 3010 Victoria, Australia; [d]Institute for Chemistry and Biochemistry, Freie Universität Berlin, 14195 Berlin, Germany; [f]Departamento de Microbiologia, Immunologia e Parasitologia, Universidade Federal de São Paulo, 04039-032 São Paulo, Brazil; [g]Institute of Biology, Humboldt University, 10117 Berlin, Germany

ABSTRACT ***Plasmodium*** **relies on actin-based motility to migrate from the site of infection and invade target cells. Using a substrate-dependent gliding locomotion, sporozoites are able to move at fast speed (1–3 μm/s). This motility relies on a minimal set of actin regulatory proteins and occurs in the absence of detectable filamentous actin (F-actin). Here we report an overexpression strategy to investigate whether perturbations of F-actin steady-state levels affect gliding locomotion and host invasion. We selected two vital *Plasmodium berghei* G-actin–binding proteins, C-CAP and profilin, in combination with three stage-specific promoters and mapped the phenotypes afforded by overexpression in all three extracellular motile stages. We show that in merozoites and ookinetes, additional expression does not impair life cycle progression. In marked contrast, overexpression of C-CAP and profilin in sporozoites impairs circular gliding motility and salivary gland invasion. The propensity for productive motility correlates with actin accumulation at the parasite tip, as revealed by combinations of an actin-stabilizing drug and transgenic parasites. Strong expression of profilin, but not C-CAP, resulted in complete life cycle arrest. Comparative overexpression is an alternative experimental genetic strategy to study essential genes and reveals effects of regulatory imbalances that are not uncovered from deletion-mutant phenotyping.**

Monitoring Editor
Laurent Blanchoin
CEA Grenoble

Received: Oct 27, 2015
Revised: May 9, 2016
Accepted: May 16, 2016

INTRODUCTION

During the complex *Plasmodium* life cycle, three extracellular stages, termed merozoites, ookinetes, and sporozoites, are tailor-made for parasite migration and host cell invasion. Many processes, including coordinated release and processing of adhesins, adhesin–substrate interactions, regulation of the actin–myosin motor complex, and formation of a moving junction at the host–parasite interface, must be carefully orchestrated for fast and efficient motility, which in turn is essential for parasite life cycle progression (Sibley, 2010). The fastest parasites are mature salivary gland–associated sporozoites. They rely on gliding motility, which is a unique form of actin-based motility, to migrate through the skin, penetrate dermal blood vessels, and eventually invade a suitable hepatocyte (Menard *et al.*, 2013; Douglas *et al.*, 2015). A hallmark of this cellular motility is an actin-myosin–dependent form of substrate-dependent locomotion (Sattler *et al.*, 2011).

Despite the central role of filament dynamics, only a limited number of known actin regulatory proteins are identified in the *Plasmodium* genomes and from proteomics analysis (Florens *et al.*, 2002; Gardner *et al.*, 2002; Hall *et al.*, 2005; Baum *et al.*, 2006;

This article was published online ahead of print in MBoC in Press (http://www.molbiolcell.org/cgi/doi/10.1091/mbc.E15-10-0734) on May 25, 2016.

*Address correspondence to: Yuko Sato (yuko@smart.mit.edu).

Abbreviations used: ADF, actin-depolymerizing factor; AMA1, apical membrane antigen 1; C-CAP, C-terminal homology domain of adenylate cyclase–associated protein; CSP, circumsporozoite protein; CTRP, circumsporozoite protein/thrombospondin–related anonymous protein–related protein; CytD, cytochalasin D; G-ABP, G-actin–binding protein; JAS, jasplakinolide.

© 2016 Sato *et al.* This article is distributed by The American Society for Cell Biology under license from the author(s). Two months after publication it is available to the public under an Attribution–Noncommercial–Share Alike 3.0 Unported Creative Commons License (http://creativecommons.org/licenses/by-nc-sa/3.0).
"ASCB®," "The American Society for Cell Biology®," and "Molecular Biology of the Cell®" are registered trademarks of The American Society for Cell Biology.

Schüler and Matuschewski, 2006; Lasonder *et al.*, 2008; Lindner *et al.*, 2013). Regulatory proteins include filamentous (F)-actin–binding proteins for nucleation, stabilization, and bundling of F-actin and globular (G)-actin–binding proteins (G-ABPs), which together control F-actin turnover (Sattler *et al.*, 2011). Known G-ABPs in *Plasmodium* parasites are actin-depolymerizing factor (ADF) 1 and 2, C-terminal homology domain of adenylate cyclase–associated protein (C-CAP), and profilin. ADF1 is essential for pathogenic blood-stage parasites, stimulates nucleotide exchange by interacting with actin monomers, and severs F-actin with low affinity (Schüler *et al.*, 2005a; Singh *et al.*, 2011; Wong *et al.*, 2014). ADF2 was reported to have similar functions as ADF1; however, deletion of *ADF2* leads to only mild defects in sporogony and liver-stage development (Doi *et al.*, 2010). C-CAP is vital for sporogony and is the strongest G-actin–sequestering protein of all *Plasmodium* actin regulators (Hliscs *et al.*, 2010; Makkonen *et al.*, 2013). Profilin is also essential for blood-stage parasites, and this protein regulates actin dynamics by sequestering actin monomers for rapid polymer formation and is stimulated by interaction with formins through its polyproline-binding residues (Baum *et al.*, 2008; Kursula *et al.*, 2008; Pino *et al.*, 2012). Of importance, a conditional knockout of profilin in the related apicomplexan parasite *Toxoplasma* ablated tachyzoite gliding motility and host cell invasion (Plattner *et al.*, 2008).

Apicomplexan actins are highly divergent from other eukaryotic actins and display relatively low sequence identity of only 75–80% (Wesseling *et al.*, 1988; Dobrowolski *et al.*, 1997). Actin I is expressed throughout the *Plasmodium* life cycle, whereas actin II is expressed predominantly in the sexual stages and during sporogonic development (Deligianni *et al.*, 2011; Lindner *et al.*, 2013; Andreadaki *et al.*, 2014). Although actin regulatory proteins have been characterized in apicomplexan parasites, the contribution of actin dynamics to cellular motility is not entirely clear. Monomeric G-actin is abundant in the parasite cytoplasm (Dobrowolski *et al.*, 1997), and the presence of stable F-actin in sporozoites is enigmatic (Kudryashev *et al.*, 2010; Angrisano *et al.*, 2012b). The apparent failure to detect microfilaments could be due to their short length, rapid turnover, and/or intrinsic instability. In vitro studies on *Plasmodium* actin showed that it rapidly hydrolyzes ATP and forms oligomers in the presence of ADP, leading to short and highly dynamic filaments (Schmitz *et al.*, 2005; Schüler *et al.*, 2005b; Sahoo *et al.*, 2006; Vahokoski *et al.*, 2014). Expression of mutant actins that recover filament stability in *Toxoplasma* greatly affected parasite motility and egress (Skillman *et al.*, 2011). Recently, actin I filaments were identified in *Plasmodium* gametocytes using superresolution microscopy, and thus F-actin seems to play a structural role in a nonmotile stage of the life cycle (Hliscs *et al.*, 2015). Together intrinsic instability of the filament population combined with a predominance of G-actin over F-actin suggests that apicomplexan actin dynamics is skewed toward G-actin in extracellular motile stages (Olshina *et al.*, 2012). Of importance, independent genetic proofs for vital functions of *Toxoplasma* actin I in host cell invasion underscore the key role(s) of parasite microfilaments in parasite propagation and life cycle progression (Dobrowolski and Sibley, 1996; Drewry and Sibley, 2015).

We hypothesized that F-actin regulation is under distinct control in the three motile *Plasmodium* stages. To study the effect of perturbed microfilament dynamics, we established a reverse genetics strategy based on an approach developed in the unicellular model organism *Saccharomyces cerevisiae* to identify genes whose overexpression confers specific phenotypes (Liu *et al.*, 1992; Sopko *et al.*, 2006). Unlike in the promoter swap strategy we previously established (Siden-Kiamos *et al.*, 2011), transgenic parasites contain an additional gene copy under the control of stage-specific promoters to achieve overexpression in distinct phases of the *Plasmodium* life cycle. The corresponding phenotype was expected to reflect regulatory imbalances and differ considerably from deletion-mutant phenotypes. Using this strategy, we addressed the influence of F-actin perturbance by overexpression of C-CAP and profilin in the three motile stages of *Plasmodium* parasites.

RESULTS

Generation of parasite lines that successfully overexpress G-actin–binding proteins in motile *Plasmodium* stages

In this study, the importance of F-actin regulation in motile *Plasmodium* stages, that is, merozoites, ookinetes, and sporozoites, was assessed by stage-specific overexpression. *AMA1*, *CTRP*, and *CSP* promoters were chosen to achieve different strengths and distinct temporal expressions in *Plasmodium berghei* parasites. Apical membrane antigen 1 (AMA1) is a transmembrane protein expressed in merozoites and sporozoites, which serves as a parasite ligand for successful host cell invasion (Triglia *et al.*, 2000; Silvie *et al.*, 2004). Circumsporozoite protein/thrombospondin–related anonymous protein–related protein (CTRP) is the TRAP-family invasin of motile ookinetes (Dessens *et al.*, 1999; Templeton *et al.*, 2000), and circumsporozoite protein (CSP) is the major surface protein of sporozoites (Dame *et al.*, 1984; Enea *et al.*, 1984).

Six integration constructs were designed to generate parasites containing the amino-terminally FLAG-tagged *C-CAP* or *profilin* and their respective 3′ untranslated regions (UTRs) under the control of the three selected promoters (Figure 1A). On a single crossover event, this fragment is predicted to insert an additional gene copy together with the positive selectable marker (*dhfr/ts*). Selected transgenic parasites were genotyped by diagnostic PCR using parasite genomic DNA as template (Supplemental Figure S1, A and B). These six transgenic parasite lines are referred to here as C-CAP^{AMA1}, C-CAP^{CTRP}, C-CAP^{CSP}, profilin^{AMA1}, profilin^{CTRP}, and profilin^{CSP}, indicating the respective promoter with a superscript.

To confirm successful overexpression by our strategy, we profiled steady-state mRNA levels of *C-CAP* and *profilin* by quantitative real-time (qRT)-PCR (Figure 1, B and C, and Supplemental Figure S2). We analyzed mRNA levels in schizonts, ookinetes, and midgut and hemocoel sporozoites. *C-CAP* and *profilin* transcripts were normalized to *HSP70/1*, an abundant and ubiquitously expressed *Plasmodium* gene (Hliscs *et al.*, 2013). Up-regulation in transgenic parasites compared with wild-type (WT) parasites was consistently higher for *C-CAP* and particularly strong in sporozoites (~1000- to 10,000-fold change; Figure 1B). Similarly, up-regulation of transgenic *profilin* mRNA was detected in all transgenic parasites, although the overexpression was less dramatic (~10- to 80-fold change; Figure 1C). Both observations are in good agreement with low *C-CAP* transcript levels found in sporozoites (Hliscs *et al.*, 2010) and adequate *profilin* transcripts present in merozoites, ookinetes, and sporozoites (Kursula *et al.*, 2008). This strategy resulted in the anticipated stage-specific overexpression of the target genes in transgenic parasite lines without critical compensatory down-regulation of the endogenous *C-CAP* and *profilin* gene expression.

Normal asexual blood-stage growth of transgenic parasites

We first confirmed expression of FLAG-tagged proteins in synchronized C-CAP^{AMA1} and profilin^{AMA1} schizonts by Western blot (Figure 2A). As predicted, immunofluorescence imaging of schizonts revealed the cytoplasmic presence of the two G-ABPs and no effect on the distribution of merozoite surface protein-1 (MSP-1), the major merozoite coat protein (Figure 2B). To quantify asexual replication

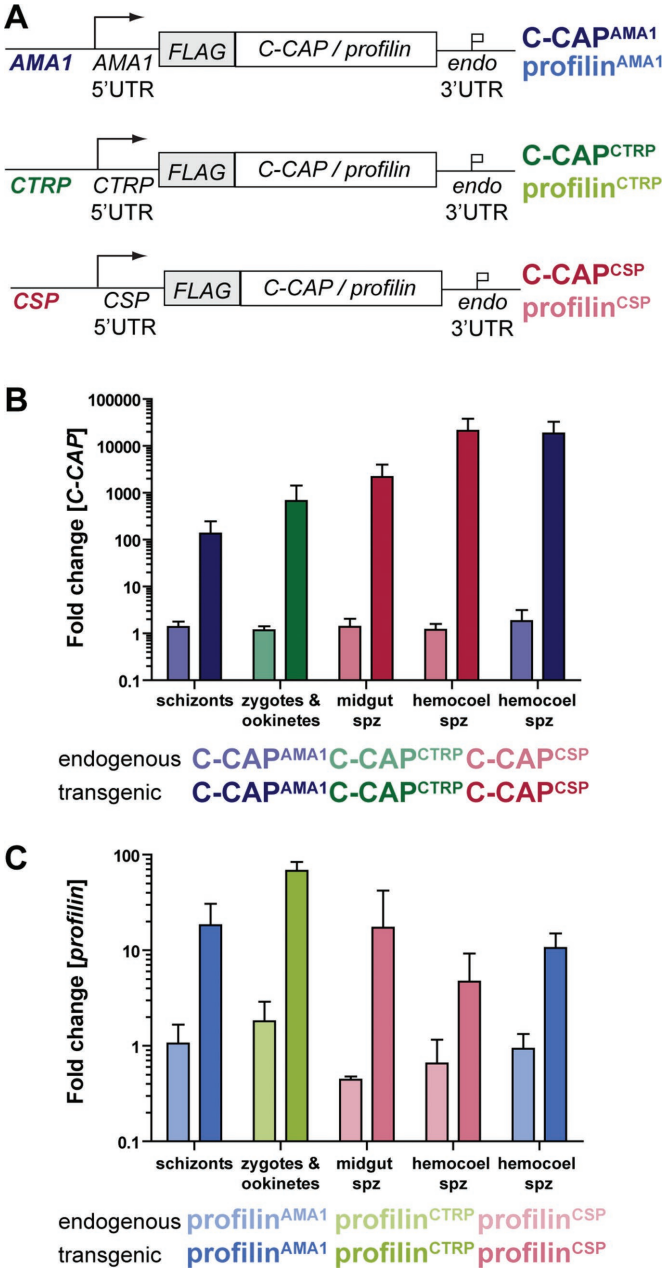

FIGURE 1: Stage-specific overexpression of C-CAP and profilin. (A) Schematic of the overexpression strategy to place C-CAP and profilin and their respective 3′ UTRs under the control of the *AMA1*, *CTRP*, or *CSP* promoter (indicated by superscripts). For detection, proteins contained an additional amino-terminal triple FLAG-tag. Parasite lines with the *AMA1* promoter are indicated in blue (top), with the *CTRP* promoter in green (center), and with the *CSP* promoter in red (bottom). Transgenic parasites overexpressing C-CAP are shown in dark colors and those overexpressing profilin in light colors. (B, C) Expression profiling of (B) *C-CAP* and (C) *profilin* in different stages of transgenic parasite lines by qRT-PCR. Fold change of relative mRNA levels of endogenous (light color) and FLAG-tagged (dark color) *C-CAP* and *profilin* in transgenic lines were compared with the abundance of the endogenous transcripts in WT parasites from the same parasite stage. Relative mRNA levels were normalized to expression levels of HSP70/1 mRNA. The results represent mean values (± SD) of three independent experiments, except for profilin^{CTRP} ookinetes and profilin^{CSP} hemocoel sporozoites ($n = 2$).

and virulence of transgenic asexual blood stages, we injected 1000 infected erythrocytes intravenously into C57BL/6 recipient mice (six each; Figure 2, C and D). The prepatent period, which is the time to microscopic detection of blood infection, was similar in all infected mice. Typically, mice became blood smear-positive at 3–4 d after parasite inoculation (Figure 2C). Growth rates of both transgenic parasite populations were similar to those of WT blood-stage parasites (Figure 2C). This result indicates that additional G-ABP expression does not perturb population expansion during blood-stage development. Of importance, severe disease onset, as measured by signature symptoms of experimental cerebral malaria (ECM), was similar in all mice and appeared 7–10 d after parasite inoculation (Figure 2D). Note that overexpression of profilin does not phenocopy a predicted loss of function, as this gene is refractory to targeted gene deletion (Kursula *et al.*, 2008). In conclusion, both G-ABPs can be overexpressed in asexual blood-stage parasites without affecting parasite virulence.

Ookinete motility can tolerate overexpression of G-ABPs

CTRP is a micronemal protein and specifically expressed in ookinetes, where it is secreted upon contact with the mosquito midgut epithelium (Dessens *et al.*, 1999; Templeton *et al.*, 2000). As expected, detection of protein expression by Western blot and immunofluorescence microscopy showed strong expression of C-CAP and profilin and localization in the cytoplasm of C-CAP^{CTRP} and profilin^{CTRP} ookinetes (Figure 3, A and B). Next, we tracked in vitro culture–derived ookinetes for motility. Both transgenic parasite lines exhibited continuous helical movement in Matrigel similar to WT ookinetes (Figure 3, C and D). Quantification of the average speed gave ~0.15 µm/s ($n = 20$), irrespective of the parasite line examined (Figure 3E). Of importance, transmission experiments by feeding infected blood to *Anopheles stephensi* mosquitoes revealed similar oocyst numbers in transgenic- and WT-infected mosquitoes (Figure 3F). Oocysts from transgenic parasites matured completely and gave rise to normal numbers of salivary gland sporozoites, in good agreement with the absence of expression of FLAG-tagged G-ABPs in C-CAP^{CTRP} and profilin^{CTRP} midgut and salivary gland sporozoites (Supplemental Figure S3). Together the data indicate no impairment of slow-migrating *Plasmodium* ookinetes by profilin or C-CAP overexpression.

Overexpression of G-ABPs in transgenic sporozoites

Next, we assessed overexpression of G-ABPs in sporozoites in four transgenic lines: C-CAP^{CSP}, C-CAP^{AMA1}, profilin^{CSP}, and profilin^{AMA1} (Figure 4). Western blot analysis of hemocoel sporozoites showed strong expression in C-CAP^{CSP}, C-CAP^{AMA1}, and profilin^{CSP} sporozoite populations, whereas a signal in profilin^{AMA1} sporozoites was faintly detected (Figure 4A). In addition, expression was confirmed in single sporozoites by immunofluorescence microscopy of hemocoel sporozoites (Figure 4, B and C). Cytoplasmic C-CAP and profilin were highly expressed in C-CAP^{CSP} and profilin^{CSP} sporozoites, whereas expression was weaker in C-CAP^{AMA1} and profilin^{AMA1} (Figure 4B). Different protein levels of C-CAP and profilin, although expression is under the control of the same promoter, might be attributable to posttranscriptional regulation, as previously shown for the pre-erythrocytic gene *UIS4* (Silvie *et al.*, 2014). Of importance, C-CAP and profilin expressions increased in C-CAP^{AMA1} and profilin^{AMA1} lines as they matured to salivary gland sporozoites (Figure 4D).

Deficiency of *Anopheles* salivary gland colonization

Next, we investigated the influence of G-ABP overexpression in transgenic sporozoites in vivo in infected *A. stephensi* mosquitoes

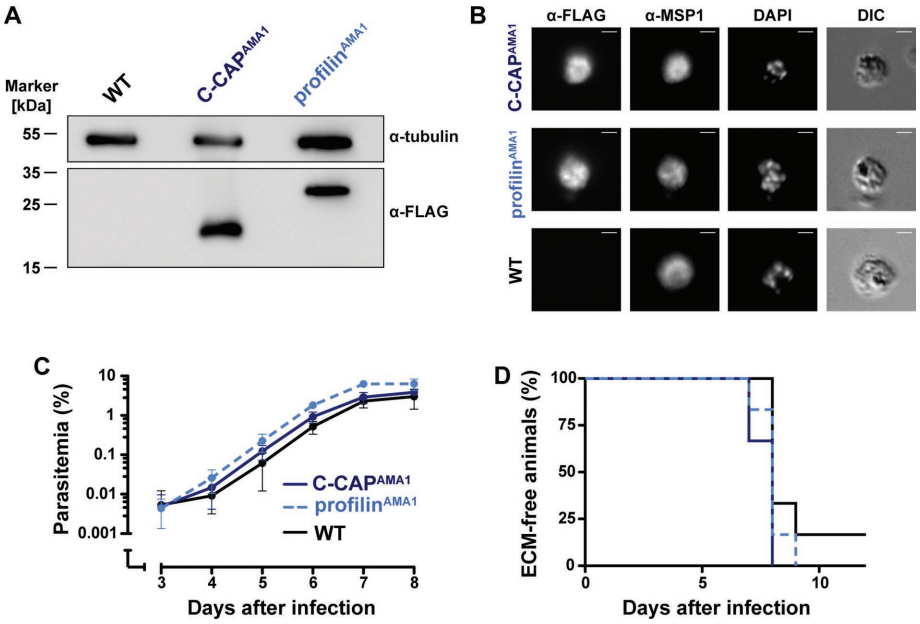

FIGURE 2: Normal growth and virulence of transgenic asexual blood-stage parasites. (A) Western blot analysis of FLAG-tagged proteins in schizonts. Samples were probed with an anti-FLAG antibody, with anti-tubulin antibodies used as control. (B) Immunofluorescence micrographs of schizonts stained with anti-FLAG (green), anti-MSP1 (red) antibodies, and 4′,6-diamidino-2-phenylindole (DAPI; blue). Bars, 2 µm. (C) Parasitemia development after intravenous injection of 1000 infected erythrocytes. Growth curves of asexual blood-stage parasites are similar in all transgenic parasite lines ($n = 6$). (D) Kaplan–Meier analysis of mice that exhibit signature symptoms of ECM. All infected animals developed ECM symptoms, except for one profilin^{AMA1}-infected mouse. Analysis by Kruskal–Wallis and Mantel–Cox tests indicated that differences are nonsignificant.

(Figure 5). Oocyst numbers were similar in all parasite lines (Figure 5A). This result implies normal zygote formation and ookinete development. Similarly, midgut and hemocoel sporozoite numbers of all four transgenic lines were comparable to those for WT infections (Figure 5, B and C). Strikingly, when salivary gland–associated sporozoites were enumerated, a strong reduction was observed in all transgenic lines compared with WT (Figure 5D). Perturbation of salivary gland invasion varied among transgenic lines. In C-CAP^{AMA1} and profilin^{AMA1} parasite lines, we typically quantified 2000–5000 salivary gland sporozoites, a twofold to fivefold reduction compared with WT sporozoites. In C-CAP^{CSP} infections, very few sporozoites were recovered from salivary glands, whereas none were detected from profilin^{CSP}-infected salivary glands. Hence sporozoites were the only one of the three motile stages impaired by overexpression of profilin and C-CAP, including in the two lines that overexpressed the target proteins under the control of the *AMA1* promoter, which did not affect blood infection (Figure 2, C and D).

Transgenic sporozoites display defects in gliding motility but not speed

To further study sporozoite motility, we isolated parasites from the mosquito hemocoel, the last phase of the developmental program where no defects were detected. Our previous work established that hemocoel sporozoites are developmentally mature, including normal infection to the mammalian host and similar immunogenicity of salivary gland sporozoites (Sato *et al.*, 2014). When hemocoel sporozoite trails with CSP deposits were quantified by immunofluorescence microscopy as a measure of circular gliding motility, we observed distinct differences in all four parasite lines (Figure 6A). First, profilin overexpression is apparently particularly detrimental, since profilin^{CSP} sporozoites displayed no signs of motility. Second, C-CAP^{CSP} sporozoites displayed either incomplete or full trails but of only a few (<10) circles. Third, C-CAP^{AMA1} and profilin^{AMA1} parasites showed a reduced number of trails compared with WT, but the majority were able to perform productive motility. Fourth, profilin^{AMA1} sporozoites overall performed better than C-CAP^{AMA1} sporozoites. Curiously, C-CAP^{AMA1} and profilin^{AMA1} gliding sporozoites displayed similar speed (~2 µm/s) as WT sporozoites (Figure 6B and Supplemental Movie S1). Transmission electron microscopy on longitudinal cross sections of sporozoites that colonized the mosquito salivary gland showed no apparent differences in organellar or cellular structures, such as the inner membrane complex (Supplemental Figure S4), indicative of normal integrity of sporozoites.

Taken together, these results show that overexpression of C-CAP and profilin disrupts the normal patterns of gliding locomotion in all four transgenic hemocoel sporozoites, but gliding speed remains unaffected in profilin^{AMA1} and C-CAP^{AMA1} sporozoite lines.

Distinct abrogation of transmission in profilin^{CSP} sporozoites

Next, we tested the capacity of transgenic hemocoel sporozoites to invade cultured hepatoma cells. Of note, profilin^{CSP} sporozoites were able to attach to hepatoma cells in a similar manner as other transgenic and WT parasites despite their incapacity to perform gliding locomotion (Supplemental Figure S5). We also observed that profilin^{AMA1} sporozoites attached with a higher frequency than WT sporozoites. Examination of the sporozoite surface of these parasites by scanning electron microscopy revealed no striking differences (Supplemental Figure S6), indicating a direct effect of elevated profilin levels on sporozoite adhesion. When hepatoma cells were infected and incubated for 2 h, all transgenic sporozoites showed reduced invasion compared with WT sporozoites (Figure 6C). In perfect agreement with the observed inability to colonize salivary glands and perform gliding motility, profilin^{CSP} sporozoites were also unable to invade hepatoma cells.

We next tested the transgenic salivary gland sporozoites for their transmission capacities and performed infection experiments using mosquitoes infected with the different transgenic parasite lines. C57BL/6 mice were exposed to mosquitoes, and the prepatent period was determined by daily microscopic examination of Giemsa-stained blood films (Figure 6D). All mice exposed to *Anopheles* mosquitoes infected with transgenic parasites became positive 3–4 d later, with the exception of mice exposed to profilin^{CSP}-infected mosquitoes. Taken together, these results show that natural transmission occurs normally even when salivary gland colonization is severely reduced, as is the case in C-CAP^{CSP} sporozoite infections (Figure 5D). Of most importance, strong overexpression of profilin, but not of C-CAP, in sporozoites resulted in ablation of sporozoite motility, cell invasion, and transmission to a new host.

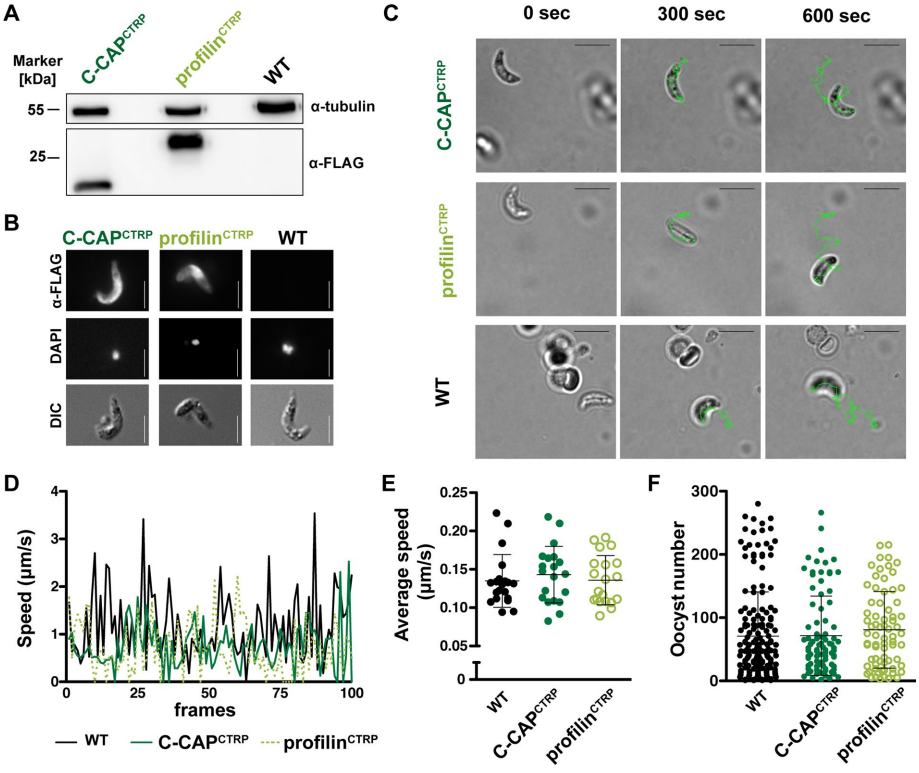

FIGURE 3: Normal ookinete motility and *Anopheles* infections in transgenic parasite lines. (A) Western blot analysis of FLAG-tagged proteins in ookinetes. Protein extracts of 100,000 purified ookinetes were separated by SDS–PAGE. Samples were probed against an anti-FLAG antibody and anti-tubulin antibody as control. (B) Immunofluorescence micrographs of ookinetes stained with anti-FLAG antibody and DAPI. Differential interference contrast images are included to display ookinetes (bars, 5 μm). (C) Time-lapse micrographs of representative ookinete at 0, 300, and 600 s. The line reflects ookinete motility in Matrigel (bars, 10 μm). (D) Representative velocities of transgenic and WT ookinetes over a recording period of 500 s. Each frame corresponds to 5 s. (E) Average speed (μm/s) was quantified from time-lapse movies ($n = 20$ each). The results represent mean values (± SD) of three independent experiments. Differences are nonsignificant (Mann–Whitney and Kruskal–Wallis tests). (F) Oocyst numbers in infected mosquitoes. The results represent mean values (± SD) of five independent natural feeding experiments.

Distinct actin I localization in transgenic sporozoites

Because overexpression of profilin and C-CAP is predicted to perturb actin dynamics, we finally assessed the distribution of actin I in sporozoites. We first quantified hemocoel sporozoite motility in the presence of the F-actin–stabilizing drug jasplakinolide (JAS; 50 nM), the inhibitor of actin polymerization cytochalasin D (CytD; 20 nM), or without drug treatment (Figure 7A). Low drug concentrations do not abrogate gliding motility and hence permit sensitive motility assays (Munter *et al.*, 2009). Under normal conditions ~30% of profilin^{AMA1} and WT sporozoites performed gliding locomotion. On addition of actin inhibitors, the motility of profilin^{AMA1} sporozoites was affected more than that of WT sporozoites. In contrast, C-CAP^{AMA1} sporozoites displayed a similar low proportion of gliding motility (~5%) regardless of the presence or absence of actin inhibitors. As expected, C-CAP^{CSP} and profilin^{CSP} sporozoites showed very little (<2%) or no motility, respectively, under all conditions tested (Figure 7A).

To visualize *Plasmodium* actin I in sporozoites, we used an antibody generated against a distinct peptide in the carboxy-terminal subdomain 4 (Supplemental Figure S7). We observed a range of staining patterns in sporozoites that could be categorized into four distinct patterns: uniform, granules, accumulation at one end, and accumulation at both ends of the sporozoite body (Figure 7B). When sporozoites were left untreated or exposed to CytD, all transgenic and WT sporozoites exhibited uniform and granular patterns, which showed no striking differences among the parasite lines (Supplemental Figure S8). Strikingly, upon JAS treatment, actin I accumulated at one or both ends, as sporozoites matured from midgut to hemocoel and on to salivary gland sporozoites (Figure 7C). Under JAS treatment, actin I distribution in C-CAP^{CSP} and profilin^{CSP} hemocoel sporozoites resembled WT midgut sporozoites, in good correlation with low or no ability to perform continuous gliding locomotion. Despite a reduction in the proportion of gliding hemocoel sporozoites (Figure 7A), actin I distribution in C-CAP^{AMA1} was indistinguishable from that for profilin^{AMA1} and WT hemocoel sporozoites under JAS treatment (Figure 7C). Of interest, we observed a reduction of WT midgut sporozoite adhesion after JAS or CytD treatment (Figure 7C and Supplemental Figure 8A), as described previously for salivary gland sporozoites (Munter *et al.*, 2009; Hegge *et al.*, 2010).

In conclusion, the combination of actin I antibody, the F-actin–stabilizing drug jasplakinolide, and transgenic parasites that overexpress the actin-binding protein profilin or C-CAP reveals actin accumulation at the sporozoite tip as a signature of productive gliding locomotion.

DISCUSSION

In this study, we report that perturbation of *Plasmodium* actin dynamics by overexpression of two actin regulatory proteins, profilin and C-CAP, specifically interferes with key sporozoite traits, namely circular gliding motility, colonization of salivary glands, and hepatocyte invasion. Accumulation of actin I at the apical and posterior ends of motile *Plasmodium* sporozoites and *Toxoplasma* tachyzoites remains the most robust indicator of the capacity to perform gliding locomotion (Wetzel *et al.*, 2003; Angrisano *et al.*, 2012a,b). The addition of transgenic *Plasmodium* sporozoites provides genetic evidence for a direct link between F-actin accumulation at the parasite tips and the frequency of gliding locomotion. Accordingly, reduced accumulation of actin I in profilin^{CSP} and C-CAP^{CSP} sporozoites, despite the presence of the F-actin–stabilizing drug JAS, is most likely due to enhanced sequestration of G-actin by the two binding proteins.

The finding that overexpression of profilin impairs sporozoite motility to a larger extent than C-CAP was unexpected. C-CAP and profilin both sequester monomeric G-actin. Purified C-CAP binds preferentially to ADP-actin monomers and does not appear to form higher–molecular weight complexes with actin (Hliscs *et al.*, 2010). Thus the function of C-CAP appears to be largely restricted to G-actin sequestration. Our observation that C-CAP^{AMA1} sporozoites retain their low frequency of gliding motility irrespective of the presence of actin inhibitors fully supports the notion that C-CAP is the strongest actin sequesterer among the *Plasmodium* actin regulators (Hliscs *et al.*, 2010). In contrast, profilin exhibits lower sequestering

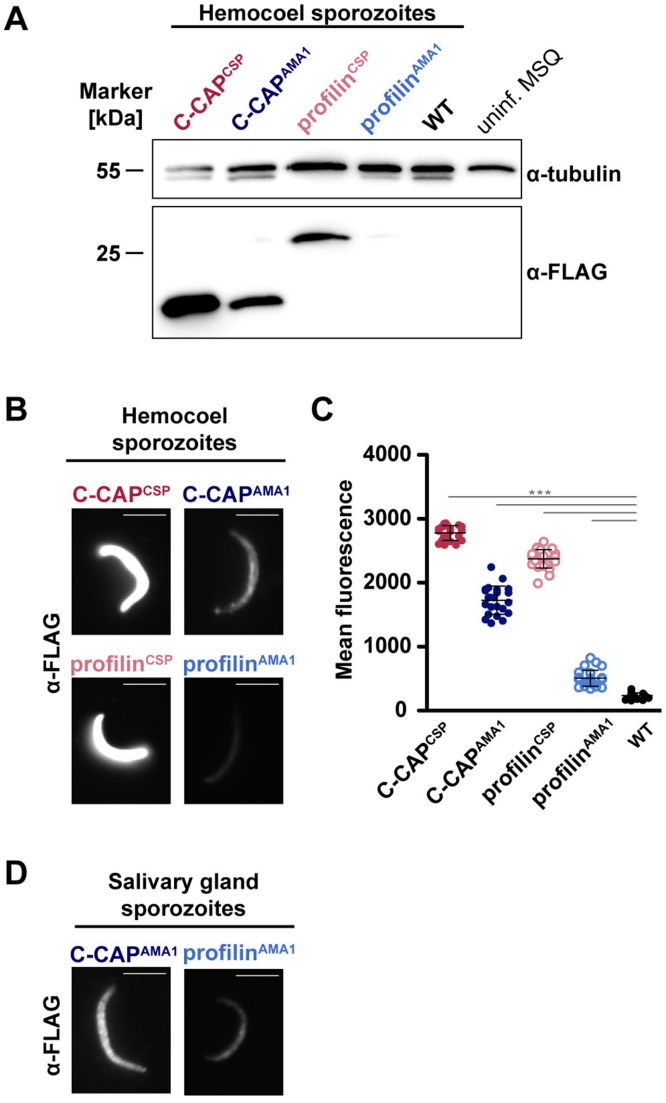

FIGURE 4: Overexpression of profilin and C-CAP in transgenic sporozoites. (A) Western blot analysis of FLAG-tagged proteins in 100,000 hemocoel sporozoites using an anti-FLAG antibody. Anti-tubulin was used as a loading control. Upper and lower bands correspond to mosquito and *Plasmodium* tubulin, respectively. uninf. MSQ, 10 uninfected female mosquitoes were loaded as a negative control. (B) Immunofluorescence micrographs of hemocoel sporozoites using an anti-FLAG antibody (bars, 5 μm). (C) Average fluorescence intensity from anti-FLAG antibody staining in sporozoites ($n \geq 20$). Mean values (± SD). ***$p < 0.001$ (Mann–Whitney test). (D) Immunofluorescence micrographs of C-CAP^{AMA1} and profilin^{AMA1} salivary gland–associated sporozoites using an anti-FLAG antibody (bars, 5 μm).

activity but accelerates nucleotide exchange and might also directly regulate elongation of F-actin via its interaction with formin (Baum *et al.*, 2008; Kursula *et al.*, 2008). It probably primarily mediates the supply of readily polymerizable G-actin. We note that a careful phenotypic analysis of gene overexpression can provide unique insights that are not uncovered by loss-of-function approaches.

Besides the prominent role of apicomplexan actin I in motility, it has also been postulated in other functions, such as vesicle trafficking and endocytosis (Lazarus *et al.*, 2008; Smythe *et al.*, 2008), ring stage morphology (Gruring *et al.*, 2011), and the organization of nuclear genes (Zhang *et al.*, 2011). Moreover, actin dynamics plays a role during intracellular parasite replication for the segregation of apicoplast, mitochondria, and secretory vesicles (Shaw and Tilney, 1999; Andenmatten *et al.*, 2013; Jacot *et al.*, 2013; Muller *et al.*, 2013; Haase *et al.*, 2015). In this study, we observed no apparent organellar and cellular defects in the morphologies of sporozoites, which were the most affected motile stage by the overexpression of G-ABPs (Supplemental Figure S4). Complete abrogation of motility and transmission of profilin^{CSP} sporozoites could be due to other binding partners of *Plasmodium* profilin, such as phosphoinositol monophosphates and phosphatidylic acid (Kursula *et al.*, 2008). Although not quantified in detail, we also noticed that profilin^{AMA1} sporozoites perform waving motion from one attached site without leaving trails. *Plasmodium* parasites are sensitive to alteration of the intracellular distribution of phosphatidylionositol-4-phosphate (McNamara *et al.*, 2013), and thus further investigations on signaling cascades that precisely map the molecular steps in moving sporozoites upon external stimuli are needed.

Our systematic comparison of six transgenic lines that overexpress two functionally related G-actin–binding proteins also establishes the concept for systematic gene overexpression in *Plasmodium* and related pathogens. Gene deletion studies established that *profilin* and *C-CAP* are vital for *Plasmodium* life cycle progression, albeit at different phases—asexual blood-stage replication and sporogony, respectively (Kursula *et al.*, 2008; Hliscs *et al.*, 2010). Perturbation of actin dynamics by overexpression of the two target proteins underscored the importance of a fine balance of microfilament regulation particularly in fast-gliding sporozoites. Of importance, gene-overexpression phenotypes did not resemble deletion-mutant phenotypes. Thus we hypothesize that systematic assessment of overexpression phenotypes will also allow annotation of genes that currently lack a loss-of-function phenotype.

We also wish to highlight two findings that further refine our molecular understanding of *Plasmodium* sporozoite biology. First, modest overexpression of G-ABPs in C-CAP^{AMA1} and profilin^{AMA1} sporozoites did not affect speed, which was measured as ~2 μm/s and is identical to that for WT sporozoites, but affected the overall proportion of productive motility. C-CAP^{AMA1} sporozoites displayed a sixfold reduction, whereas profilin^{AMA1} sporozoites move at least as actively as WT sporozoites. Thus the proportion of lasting circular and productive motility does not correlate with speed and fully supports the notion of complete maturation of hemocoel sporozoites, despite a lower proportion of continuous gliding locomotion (Sato *et al.*, 2014). Second, low rates of salivary gland colonization do not predict the success of natural transmission by *Anopheles* mosquito bite. Prepatent period and infection by exposure to C-CAP^{CSP}–infected *Anopheles* mosquitoes was indistinguishable from WT infections, despite a dramatic reduction in salivary gland–associated sporozoites. The apparent strong compensation of a transmission bottleneck, albeit plausible, has considerable implications for the design of transmission-blocking strategies. Our results show that a 10-fold reduction in salivary gland sporozoite numbers can result in a perfectly unaltered reinfection of the mammalian host, highlighting the need for near-complete life cycle arrest in the mosquito vector for any transmission-blocking intervention strategy.

In conclusion, our study provides genetic evidence for the unique importance of fine-tuning microfilament dynamics in gliding motility and natural transmission of *Plasmodium* sporozoites. Host switch from mosquito vector to the mammalian host is particularly sensitive to F-actin perturbations and other phases of the life cycle, including ookinete penetration of the mosquito midgut epithelium and merozoite invasion of host erythrocytes, appear to be less susceptible to biological perturbation. This finding also highlights

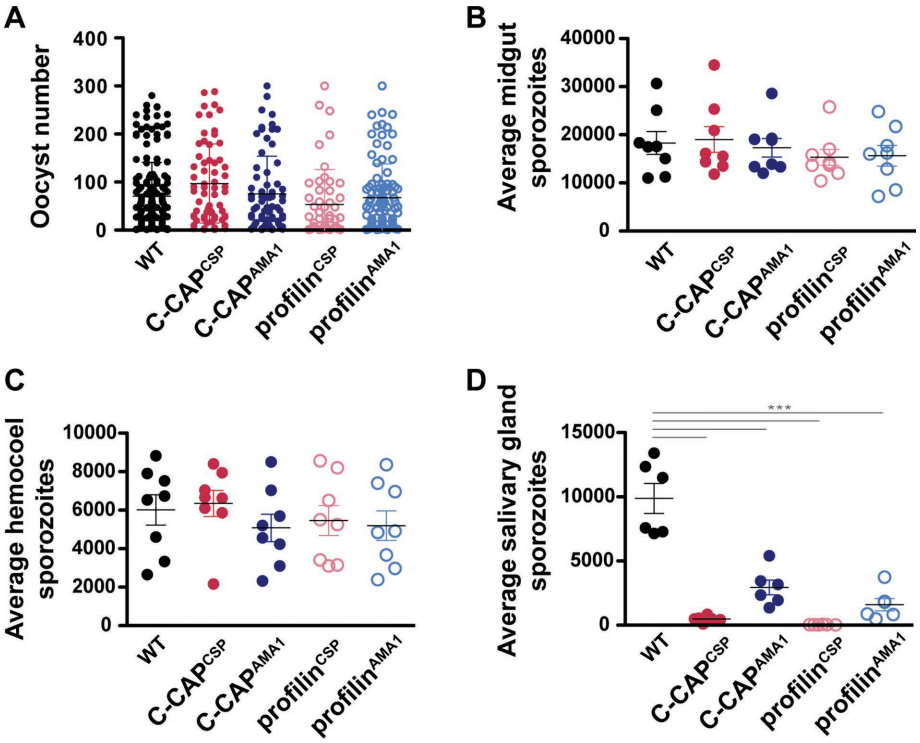

FIGURE 5: Transgenic sporozoites are impaired in colonization of *Anopheles* salivary glands. Mean values (± SD) from at least six independent experiments. (A) Oocyst numbers per mosquito. Differences are nonsignificant (Kruskal–Wallis test). (B) Average midgut sporozoites per mosquito from >160 infected mosquitoes. Differences are nonsignificant (Kruskal–Wallis test). (C) Average hemocoel sporozoites per mosquito from >300 infected mosquitoes. Differences are nonsignificant (Kruskal–Wallis test). (D) Average salivary gland sporozoites per mosquito from >80 infected mosquitoes. ***$p < 0.001$ (Kruskal–Wallis test).

Plasmodium sporozoites as particularly vulnerable to targeted intervention strategies aiming at exploiting our increasing knowledge on the molecular mechanisms of actin/myosin-based motility in apicomplexan parasites. Moreover, assessment of an overexpression phenotype is an experimental alternative to classical or conditional loss-of-function approaches in *Plasmodium* and likely also in related apicomplexan parasites and other genetically tractable pathogens.

MATERIALS AND METHODS

Experimental animals

All animal work was conducted in accordance with the German Tierschutzgesetz in der Fassung von 18. Mai 2006 (BGB1. I S. 1207), which implements the Directive 86/609/EEC from the European Union and the European Convention for the protection of vertebrate animals used for experimental and other scientific purposes. The protocol was approved by the ethics committee of the Max Planck Institute for Infection Biology and the Berlin state authorities (Landesamt für Gesundheit und Soziales regulation G0469/09). Female C57BL/6 and NMRI mice were obtained from Charles River Laboratories.

Generation of transgenic parasites

The promoters of *AMA1*, *CTRP*, and *CSP* were used to overexpress either *P. berghei* C-CAP (PBANKA 020800; gi: 225734413) or profilin (PBANKA_083300; gi: 239977531) in addition to the respective endogenous gene locus. Promoter regions and 5′ UTRs were cloned upstream of a triple FLAG-tag fused to the respective coding sequence and cognate 3′ UTR. The expression plasmids were linearized within the open reading frames by restriction enzymes (*Bst*BI for C-CAP; *Bsa*BI for profilin) and introduced into the *P. berghei* (strain ANKA) genome by single-crossover homologous recombination. Positive selection of recombinant parasites was done by oral uptake of pyrimethamine. Successful gene targeting was validated by diagnostic PCR. All primers used are listed in Supplemental Table S1.

Transcript detection

Total RNA was extracted from parasites (mixed ookinetes and zygotes, sporozoites, and schizonts) preserved in TRIzol reagent (Thermo Fisher Scientific, Darmstadt, Germany) according to the manufacturer's instructions. cDNA was synthesized from 0.5–1 µg of total RNA (RETROscript kit; Thermo Fisher Scientific), and quantitative PCR was performed with StepOnePlus using Power SYBR Green PCR Master Mix (Thermo Fisher Scientific). The assay was performed in triplicate with the reaction setting described previously (Ganter *et al.*, 2015). Endogenous as well as FLAG-tagged transcripts of *C-CAP* and *profilin* were normalized to the abundance of *HSP70/1* mRNA, and fold change was calculated with respect to endogenous *C-CAP* and *profilin* mRNA in the respective stages of WT parasites. All primers used for qRT-PCR are listed in Supplemental Table S2, and primer binding sites are given in Supplemental Figure S2.

Protein detection

Successful protein overexpression of C-CAP and profilin was analyzed by Western blot and immunofluorescence (IFA) using a monoclonal anti-FLAG antibody (clone M2; Sigma-Aldrich) due to the lack of antibodies specific to *P. berghei* profilin and C-CAP. Protein extracts were prepared from in vitro–cultured schizonts from an infected mouse, 100,000 in vitro cultured ookinetes, or 200,000 sporozoites isolated from infected *A. stephensi* mosquitoes and separated by SDS–PAGE. Monoclonal anti-tubulin antibody (clone B-5-1-2; Sigma-Aldrich, Darmstadt, Germany) was used as control. Bound antibodies were detected with secondary goat anti-mouse antibodies coupled to horseradish peroxidase (GE Healthcare, Berlin, Germany) and visualized using the ECL detection kit (GE Healthcare). IFAs were performed with 5 µl of purified schizonts, 10,000 ookinetes, or 8000 sporozoites, which were allowed to settle on poly-L-lysine–coated cover slips in 24-well plates. Samples were fixed with 4% paraformaldehyde (PFA), permeabilized with 0.2% Triton X-100, and labeled with the anti-FLAG antibody, followed by anti-mouse Alexa Fluor 488–coupled goat antibody (Thermo Fisher Scientific). For schizonts, parasites were also stained by anti–MSP-1 antibody (3D7 strain MSP1-42) with secondary anti-rabbit Alexa Fluor 548–coupled goat antibody (Thermo Fisher Scientific). Fluorescence intensity was quantified from microscopic images using ImageJ software (Schneider *et al.*, 2012).

Blood-stage infection

For in vitro cultivation of schizonts, blood with 2–5% parasitemia was collected from NMRI mice and incubated in schizont medium for

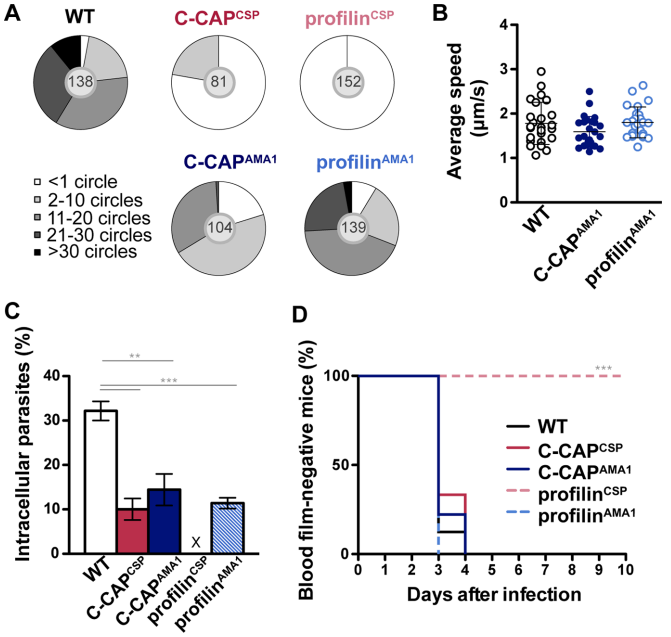

FIGURE 6: Strong overexpression of profilin abrogates gliding motility, invasion, and natural transmission. (A) Quantification of trails deposited by gliding sporozoites (categories: <1, 2–10, 11–20, 21–30, and >30). Number within the gray circle in each pie diagrams indicates total sporozoite number. (B) In vitro speed tracking of motile sporozoites. The average speed (µm/s) was quantified from representative hemocoel sporozoites ($n = 25$). Data shown are mean speed (± SD) from three independent experiments. Differences are nonsignificant (Kruskal–Wallis test). (C) Sporozoite invasion of hepatoma cells. × denotes inability to invade in profilin^{CSP} sporozoites. The results represent mean values (± SD) of three independent experiments with two samples each. $^{**}p < 0.01$; $^{***}p < 0.001$ (unpaired *t* test). (D) Malaria transmission by mosquito bites. C57BL/6 mice were exposed to 10 infected mosquitoes, and the prepatent period was monitored by daily microscopic examination of Giemsa-stained blood films. The difference of profilin^{CSP} infection to all the infections was significant.$^{***}p < 0.001$ (Mantel–Cox test).

A Gliding sporozoites

	WT	C-CAP^{CSP}	C-CAP^{AMA1}	profilin^{CSP}	profilin^{AMA1}
---	33% (41/125)	2% (3/156)	5% (8/158)	0% (0/173)	33% (33/100)
+ JAS	12% (25/218)	0% (0/149)	4% (6/149)	0% (0/98)	5% (5/105)
+ CytD	18% (21/118)	1% (1/121)	8% (10/127)	0% (0/115)	8% (11/134)

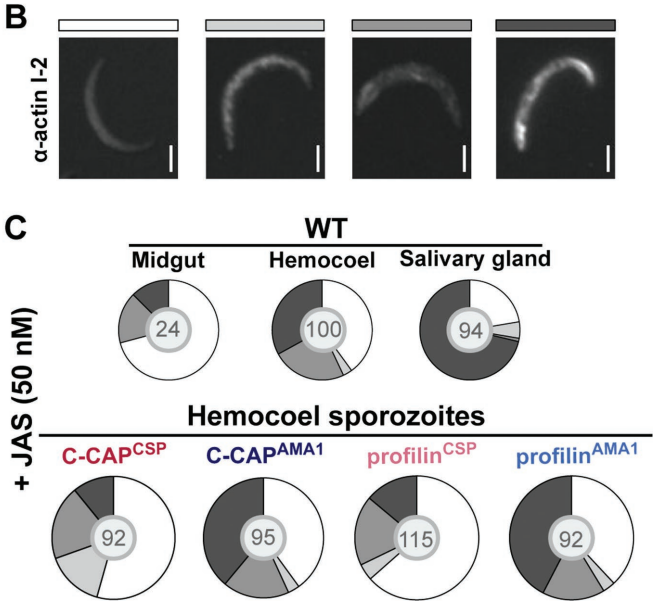

FIGURE 7: Distinct localization of actin I in motile sporozoites. (A) Percentage of gliding hemocoel sporozoites in the presence of 50 nM JAS, 20 nM CytD, or solvent control. Motility was quantified from immunofluorescence micrographs and scored as gliders when a trail of full circle was observed. Numbers in brackets are gliders out of total sporozoites. No trails were observed in profilin^{CSP} hemocoel sporozoites under all conditions tested. (B) Immunofluorescence micrographs of JAS-treated WT hemocoel sporozoites stained with an anti–*P. berghei* actin I-2 antibody. Four distinct patterns were recognized (labeled in four shades of gray on top of the images). Bars, 1 µm. (C) Quantification of actin I localization in WT midgut, hemocoel, and salivary gland sporozoites (top) and transgenic hemocoel sporozoites (bottom). All samples were treated with 50 nM JAS and quantified based on the four categories. Numbers in the gray circle are total sporozoites.

18 h at 37°C in a low-oxygen atmosphere under constant shaking. Schizonts were purified by one-step Nycodenz density gradient centrifugation (Janse *et al.*, 2006). A total of 1000 infected erythrocytes were injected intravenously into C57BL/6 mice (six each). Microscopic examination of Giemsa-stained blood smears was performed daily to determine parasitemia. During the analysis, development of signature symptoms of ECM was carefully monitored. Mice were diagnosed with onset of ECM if they showed behavioral and functional abnormalities such as ataxia, paralysis, or convulsions (Lackner *et al.*, 2006). Mice were killed immediately after a diagnosis of ECM.

Ookinete assays

Ookinetes were cultured from blood of NMRI mice infected with high gametocytemia at 20°C (Siden-Kiamos *et al.*, 2006). Ookinetes were purified using anti-P28 antibody–coated Dynabeads and a magnet (Thermo Fisher Scientific). For time-lapsed videos, purified ookinetes were mixed with Matrigel (BD Biosciences, Heidelberg, Germany) and spotted onto a Vaseline-rimmed coverslip. Speed of individual ookinetes was recorded by time-lapse video microscopy using a Zeiss Axiovert 200M microscope (Zeiss, Oberkochen, Germany) and the Volocity program (1 frame/5 s for 10 min). Speed was calculated by manually tracking at the apical end using a manual tracking plug-in of ImageJ.

Anopheles infections

A. stephensi mosquitoes were raised at 20°C in 80% humidity under a 14-h light/10-h dark cycle. Blood feeding and mosquito dissection were performed as described previously (Vanderberg, 1975). Oocysts were quantified from dissected midgut 10 d after an infectious blood meal by epifluorescence microscopy. Midgut, hemocoel, and salivary gland sporozoites were isolated from infected mosquitoes as described (Sato *et al.*, 2014).

Sporozoite assays

To quantify sporozoite motility, eight-well chamber glass slides were precoated with RPMI medium containing 3% bovine serum albumin (BSA). A total of 8000 sporozoites were dissected in RPMI–3% BSA and incubated for 45 min at 37°C. After fixation with 4% PFA, sporozoites and trails were detected using a monoclonal anti-*P. berghei*

CSP antibody (Potocnjak *et al.*, 1980). For drug inhibition studies, either 50 nM JAS (Thermo Fisher Scientific) or 20 nM CytD (Sigma-Aldrich) was added. To record gliding sporozoites, 50,000 sporozoites in 20 µl of RPMI–3% BSA were placed in the center of an imaging dish (µ-Dish, 35 mm, 10w Grid-500; ibidi, Planegg, Germany), allowed to settle, and recorded by time-lapse video microscopy using a Zeiss Axiovert 200M microscope equipped with a heated chamber and the Volocity program (1 frame/s for 2 min). To quantify sporozoite adhesion to and entry into hepatoma cells, 8000 sporozoites in 120 µl of DMEM complete were added to eight-well-chamber glass slides previously seeded with Huh7 hepatoma cells. Cells were incubated for 30 min at room temperature, followed by 90 min at 37°C (5% CO_2). After medium removal, cells and adhering sporozoites were fixed with 4% PFA. A two-color invasion assay was used as described (Renia *et al.*, 1988).

Electron microscopy

Samples for transmission electron microscopy (TEM) were prepared by fixing colonized mosquito salivary glands in 4% PFA on eight-well-chamber glass slides and embedding them in 2% agarose solution for easier handling. Samples were postfixed in 2.5% glutaraldehyde, contrasted with 0.5% osmium tetroxide, tannic acid, and 2% uranyl-acetate, dehydrated in a graded ethanol series, and infiltrated in styrene and three changes of epoxy resin for several hours. They were then embedded in epoxy and heat-cured overnight. Sections of the salivary glands were made with an Ultracut-R ultramicrotome (Leica Microsystems, Wetzlar, Germany) and retrieved with copper grids. TEM samples were analyzed in a LEO 912 (Zeiss) equipped with a Cantega bottom-mounted digital camera (SIS-Olympus, Münster, Germany).

To perform scanning electron microscopy of hemocoel sporozoites, parasites were deposited onto BSA-coated glass slides and incubated for 45 min at 37°C. Samples were fixed in 2.5% glutaraldehyde and postfixed in 0.5% osmium tetroxide, tannic acid, and osmium tetroxide. The samples were then dehydrated in a graded ethanol series, dried in CO_2 at critical point, and vacuum coated with 3-nm carbon-platinum. Imaging was performed in a LEO 1550 (Zeiss) at 15-kV acceleration voltages.

Natural transmission experiments

Natural transmission of sporozoites from the mosquito vector to the mammalian host was tested by exposure of C57BL/6 mice to infected *Anopheles* mosquitoes. Ten infected mosquitoes were allowed to feed for 15 min on anesthetized mice. Appearance of blood-stage parasites was done by daily microscopic examination of Giemsa-stained blood films.

Generation of an anti–actin I serum and detection in sporozoites

We previously reported an antiserum that detects filamentous actin I in *P. berghei* ookinetes, which was generated against a synthetic peptide corresponding to amino acids 16–30 in subdomain 1 of actin I (Siden-Kiamos *et al.*, 2012). Because this reagent did not detect a signal in sporozoites, we raised an antiserum against a synthetic peptide from actin I corresponding to the polypeptide NH_2-FDEEMKTSEQSSDIEK-CO_2, corresponding to amino acids 224–238 in subdomain 4, named AbactinI-2; this peptide is sufficiently divergent from the *Plasmodium* isoform actin II (Deligianni *et al.*, 2011). For IFA, fixed and permeabilized sporozoites were incubated with AbactinI-2, followed by anti-rabbit Alexa Fluor 546–coupled goat antibody (Thermo Fisher Scientific). Fluorescence signals from sporozoite samples were assigned to one of four categories: uniform, granular, accumulation at one tip, and accumulation at both tips.

Statistical analysis

Statistics was assessed using GraphPad Prism 5 (GraphPad Software, La Jolla, CA). Statistical significance was calculated using a Mann–Whitney test or an unpaired *t* test. $p < 0.05$ was considered significant. Survival curves were compared by using the log rank (Mantel–Cox) test. The Kruskal–Wallis test was performed to compare the significance of dependent data.

ACKNOWLEDGMENTS

We thank Friedrich Frischknecht for fruitful discussions and critical reading of the manuscript and Inga Siden Kiamos for testing the antibody against *P. berghei* actin I-2. This work was supported by the Max Planck Society and in part by the EviMalaR Network of Excellence (#34). Y.S. was supported by the ZIBI Graduate School Berlin Research in Infection Biology and Immunology. J.D. was supported by the German Research Foundation.

REFERENCES

Andenmatten N, Egarter S, Jackson AJ, Jullien N, Herman J-P, Meissner M (2013). Conditional genome engineering in *Toxoplasma gondii* uncovers alternative invasion mechanisms. Nat Methods 10, 125–127.

Andreadaki M, Morgan RN, Deligianni E, Kooij TW, Santos JM, Spanos L, Matuschewski K, Louis C, Mair GR, Siden-Kiamos I (2014). Genetic crosses and complementation reveal essential functions for the *Plasmodium* stage-specific actin 2 in sporogonic development. Cell Microbiol 16, 751–767.

Angrisano F, Delves MJ, Sturm A, Mollard V, McFadden GI, Sinden RE, Baum J (2012a). A GFP-actin reporter line to explore microfilament dynamics across the malaria parasite lifecycle. Mol Biochem Parasitol 182, 93–96.

Angrisano F, Riglar DT, Sturm A, Volz JC, Delves MJ, Zuccala ES, Turnbull L, Dekiwadia C, Olshina MA, Marapana DS, *et al.* (2012b). Spatial localisation of actin filaments across developmental stages of the malaria parasite. PLoS One 7, e32188.

Baum J, Papenfuss AT, Baum B, Speed TP, Cowman AF (2006). Regulation of apicomplexan actin-based motility. Nat Rev Microbiol 4, 621–628.

Baum J, Tonkin CJ, Paul AS, Rug M, Smith BJ, Gould SB, Richard D, Pollard TD, Cowman AF (2008). A malaria parasite formin regulates actin polymerization and localizes to the parasite-erythrocyte moving junction during invasion. Cell Host Microbe 3, 188–198.

Dame JB, Williams JL, McCutchan TF, Weber JL, Wirtz RA, Hockmeyer WT, Maloy WL, Haynes JD, Schneider I, Roberts D, *et al.* (1984). Structure of the gene encoding the immunodominant surface antigen on the sporozoite of the human malaria parasite *Plasmodium falciparum*. Science 225, 593–599.

Deligianni E, Morgan RN, Bertuccini L, Kooij TW, Laforge A, Nahar C, Poulakakis N, Schüler H, Louis C, Matuschewski K, *et al.* (2011). Critical role for a stage-specific actin in male exflagellation of the malaria parasite. Cell Microbiol 13, 1714–1730.

Dessens JT, Beetsma AL, Dimopoulos G, Wengelnik K, Crisanti A, Kafatos FC, Sinden RE (1999). CTRP is essential for mosquito infection by malaria ookinetes. EMBO J 18, 6221–6227.

Dobrowolski JM, Niesman IR, Sibley LD (1997). Actin in the parasite *Toxoplasma gondii* is encoded by a single copy gene, ACT1, and exists primarily in a globular form. Cell Motil Cytoskeleton 37, 253–262.

Dobrowolski JM, Sibley LD (1996). *Toxoplasma* invasion of mammalian cells is powered by the actin cytoskeleton of the parasite. Cell 84, 933–939.

Doi Y, Shinzawa N, Fukumoto S, Okano H, Kanuka H (2010). ADF2 is required for transformation of the ookinete and sporozoite in malaria parasite development. Biochem Biophys Res Commun 397, 668–672.

Douglas RG, Amino R, Sinnis P, Frischknecht F (2015). Active migration and passive transport of malaria parasites. Trends Parasitol 31, 357–362.

Drewry LL, Sibley LD (2015). *Toxoplasma* actin is required for efficient host cell invasion. mBio 6, e00557–00515.

Enea V, Ellis J, Zavala F, Arnot DE, Asavanich A, Masuda A, Quakyi I, Nussenzweig RS (1984). DNA cloning of *Plasmodium falciparum*

circumsporozoite gene: amino acid sequence of repetitive epitope. Science 225, 628–630.
Florens L, Washburn MP, Raine JD, Anthony RM, Grainger M, Haynes JD, Moch JK, Muster N, Sacci JB, Tabb DL, *et al.* (2002). A proteomic view of the *Plasmodium falciparum* life cycle. Nature 419, 520–526.
Ganter M, Rizopoulos Z, Schüler H, Matuschewski K (2015). Pivotal and distinct role for *Plasmodium* actin capping protein alpha during blood infection of the malaria parasite. Mol Microbiol 96, 84–94.
Gardner MJ, Hall N, Fung E, White O, Berriman M, Hyman RW, Carlton JM, Pain A, Nelson KE, Bowman S, *et al.* (2002). Genome sequence of the human malaria parasite *Plasmodium falciparum*. Nature 419, 498–511.
Gruring C, Heiber A, Kruse F, Ungefehr J, Gilberger T-W, Spielmann T (2011). Development and host cell modifications of *Plasmodium falciparum* blood stages in four dimensions. Nat Commun 2, 165.
Haase S, Zimmermann D, Olshina MA, Wilkinson M, Fisher F, Tan YH, Stewart RJ, Tonkin CJ, Wong W, Kovar DR, Baum J (2015). Disassembly activities of actin depolymerization factor (ADF) is associated with distinct cellular processes in apicomplexan parasites. Mol Biol Cell 26, 3001–3012.
Hall N, Karras M, Raine JD, Carlton JM, Kooij TW, Berriman M, Florens L, Janssen CS, Pain A, Christophides GK, *et al.* (2005). A comprehensive survey of the *Plasmodium* life cycle by genomic, transcriptomic, and proteomic analyses. Science 307, 82–86.
Hegge S, Munter S, Steinbuchel M, Heiss K, Engel U, Matuschewski K, Frischknecht F (2010). Multistep adhesion of *Plasmodium* sporozoites. FASEB J 24, 2222–2234.
Hliscs M, Millet C, Dixon MW, Siden-Kiamos I, McMillan P, Tilley L (2015). Organization and function of an actin cytoskeleton in *Plasmodium falciparum* gametocytes. Cell Microbiol 17, 207–225.
Hliscs M, Nahar C, Frischknecht F, Matuschewski K (2013). Expression profiling of *Plasmodium berghei* HSP70 genes for generation of bright red fluorescent parasites. PLoS One 8, e72771.
Hliscs M, Sattler JM, Tempel W, Artz JD, Dong A, Hui R, Matuschewski K, Schüler H (2010). Structure and function of a G-actin sequestering protein with a vital role in malaria oocyst development inside the mosquito vector. J Biol Chem 285, 11572–11583.
Jacot D, Daher W, Soldati-Favre D (2013). *Toxoplasma gondii* myosin F, an essential motor for centrosomes positioning and apicoplast inheritance. EMBO J 32, 1702–1716.
Janse CJ, Franke-Fayard B, Mair GR, Ramesar J, Thiel C, Engelmann S, Matuschewski K, van Gemert GJ, Sauerwein RW, Waters AP, *et al.* (2006). High efficiency transfection of *Plasmodium berghei* facilitates novel selection procedures. Mol Biochem Parasitol 145, 60–70.
Kudryashev M, Lepper S, Baumeister W, Cyrklaff M, Frischknecht F (2010). Geometric constrains for detecting short actin filaments by cryogenic electron tomography. BMC Biophys 3, 6.
Kursula I, Kursula P, Ganter M, Panjikar S, Matuschewski K, Schüler H (2008). Structural basis for parasite-specific functions of the divergent profilin of *Plasmodium falciparum*. Structure 16, 1638–1648.
Lackner P, Beer R, Heussler V, Goebel G, Rudzki D, Helbok R, Tannich E, Schmutzhard E (2006). Behavioural and histopathological alterations in mice with cerebral malaria. Neuropathol Appl Neurobiol 32, 177–188.
Lasonder E, Janse CJ, van Gemert G-J, Mair GR, Vermunt AM, Douradinha BG, van Noort V, Huynen MA, Luty AJ, Kroeze H, *et al.* (2008). Proteomic profiling of *Plasmodium* sporozoite maturation identifies new proteins essential for parasite development and infectivity. PLoS Pathog 4, e1000195.
Lazarus MD, Schneider TG, Taraschi TF (2008). A new model for hemoglobin ingestion and transport by the human malaria parasite *Plasmodium falciparum*. J Cell Sci 121, 1937–1949.
Lindner SE, Swearingen KE, Harupa A, Vaughan AM, Sinnis P, Moritz RL, Kappe SH (2013). Total and putative surface proteomics of malaria parasite salivary gland sporozoites. Mol Cell Proteomics 12, 1127–1143.
Liu H, Krizek J, Bretscher A (1992). Construction of a GAL1-regulated yeast cDNA expression library and its application to the identification of genes whose overexpression causes lethality in yeast. Genetics 132, 665–673.
Makkonen M, Bertling E, Chebotareva NA, Baum J, Lappalainen P (2013). Mammalian and malaria parasite cyclase-associated proteins catalyze nucleotide exchange on G-actin through a conserved mechanism. J Biol Chem 288, 984–994.
McNamara CW, Lee MC, Lim CS, Lim SH, Roland J, Nagle A, Simon O, Yeung BK, Chatterjee AK, McCormack SL, *et al.* (2013). Targeting *Plasmodium* PI (4) K to eliminate malaria. Nature 504, 248–253.
Menard R, Tavares J, Cockburn I, Markus M, Zavala F, Amino R (2013). Looking under the skin: the first steps in malarial infection and immunity. Nat Rev Microbiol 11, 701–712.
Muller C, Klages N, Jacot D, Santos JM, Cabrera A, Gilberger TW, Dubremetz J-F, Soldati-Favre D (2013). The *Toxoplasma* protein ARO mediates the apical positioning of rhoptry organelles, a prerequisite for host cell invasion. Cell Host Microbe 13, 289–301.
Munter S, Sabass B, Selhuber-Unkel C, Kudryashev M, Hegge S, Engel U, Spatz JP, Matuschewski K, Schwarz US, Frischknecht F (2009). *Plasmodium* sporozoite motility is modulated by the turnover of discrete adhesion sites. Cell Host Microbe 6, 551–562.
Olshina MA, Wong W, Baum J (2012). Holding back the microfilament: Structural insights into actin and the actin-monomer-binding proteins of apicomplexan parasites. IUBMB Life 64, 370–377.
Pino P, Sebastian S, Kim EA, Bush E, Brochet M, Volkmann K, Kozlowski E, Llinas M, Billker O, Soldati-Favre D (2012). A tetracycline-repressible transactivator system to study essential genes in malaria parasites. Cell Host Microbe 12, 824–834.
Plattner F, Yarovinsky F, Romero S, Didry D, Carlier M-F, Sher A, Soldati-Favre D (2008). *Toxoplasma* profilin is essential for host cell invasion and TLR11-dependent induction of an interleukin-12 response. Cell Host Microbe 3, 77–87.
Potocnjak P, Yoshida N, Nussenzweig RS, Nussenzweig V (1980). Monovalent fragments (Fab) of monoclonal antibodies to a sporozoite surface antigen (*Pb*44) protect mice against malarial infection. J Exp Med 151, 1504–1513.
Renia L, Miltgen F, Charoenvit Y, Ponnudurai T, Verhave JP, Collins WE, Mazier D (1988). Malaria sporozoite penetration A new approach by double staining. J Immunol Methods 112, 201–205.
Sahoo N, Beatty W, Heuser J, Sept D, Sibley LD (2006). Unusual kinetic and structural properties control rapid assembly and turnover of actin in the parasite *Toxoplasma gondii*. Mol Biol Cell 17, 895–906.
Sato Y, Montagna GN, Matuschewski K (2014). *Plasmodium berghei* sporozoites acquire virulence and immunogenicity during mosquito hemocoel transit. Infect Immun 82, 1164–1172.
Sattler JM, Ganter M, Hliscs M, Matuschewski K, Schüler H (2011). Actin regulation in the malaria parasite. Eur J Cell Biol 90, 966–971.
Schmitz S, Grainger M, Howell S, Calder LJ, Gaeb M, Pinder JC, Holder AA, Veigel C (2005). Malaria parasite actin filaments are very short. J Mol Biol 349, 113–125.
Schneider CA, Rasband WS, Eliceiri KW (2012). NIH Image to ImageJ: 25 years of image analysis. Nat Methods 9, 671–675.
Schüler H, Matuschewski K (2006). Regulation of apicomplexan microfilament dynamics by a minimal set of actin-binding proteins. Traffic 7, 1433–1439.
Schüler H, Mueller A-K, Matuschewski K (2005a). A *Plasmodium* actin-depolymerizing factor that binds exclusively to actin monomers. Mol Biol Cell 16, 4013–4023.
Schüler H, Mueller A-K, Matuschewski K (2005b). Unusual properties of *Plasmodium falciparum* actin: new insights into microfilament dynamics of apicomplexan parasites. FEBS Lett 579, 655–660.
Shaw MK, Tilney LG (1999). Induction of an acrosomal process in *Toxoplasma gondii*: visualization of actin filaments in a protozoan parasite. Proc Natl Acad Sci USA 96, 9095–9099.
Sibley LD (2010). How apicomplexan parasites move in and out of cells. Curr Opin Biotechnol 21, 592–598.
Siden-Kiamos I, Ganter M, Kunze A, Hliscs M, Steinbuchel M, Mendoza J, Sinden RE, Louis C, Matuschewski K (2011). Stage-specific depletion of myosin A supports an essential role in motility of malarial ookinetes. Cell Microbiol 13, 1996–2006.
Siden-Kiamos I, Louis C, Matuschewski K (2012). Evidence for filamentous actin in ookinetes of a malarial parasite. Mol Biochem Parasitol 181, 186–189.
Siden-Kiamos I, Pinder JC, Louis C (2006). Involvement of actin and myosins in *Plasmodium berghei* ookinete motility. Mol Biochem Parasitol 150, 308–317.
Silvie O, Briquet S, Müller K, Manzoni G, Matuschewski K (2014). Post-transcriptional silencing of UIS4 in *Plasmodium berghei* sporozoites is important for host switch. Mol Microbiol 91, 1200–1213.
Silvie O, Franetich J-F, Charrin S, Mueller MS, Siau A, Bodescot M, Rubinstein E, Hannoun L, Charoenvit Y, Kocken CH, *et al.* (2004). A role for apical membrane antigen 1 during invasion of hepatocytes by *Plasmodium falciparum* sporozoites. J Biol Chem 279, 9490–9496.
Singh BK, Sattler JM, Chatterjee M, Huttu J, Schüler H, Kursula I (2011). Crystal structures explain functional differences in the two actin depolymerization factors of the malaria parasite. J Biol Chem 286, 28256–28264.

Skillman KM, Diraviyam K, Khan A, Tang K, Sept D, Sibley LD (2011). Evolutionarily divergent, unstable filamentous actin is essential for gliding motility in apicomplexan parasites. PLoS Pathog 7, e1002280.

Smythe WA, Joiner KA, Hoppe HC (2008). Actin is required for endocytic trafficking in the malaria parasite *Plasmodium falciparum*. Cell Microbiol 10, 452–464.

Sopko R, Huang D, Preston N, Chua G, Papp B, Kafadar K, Snyder M, Oliver SG, Cyert M, Hughes TR (2006). Mapping pathways and phenotypes by systematic gene overexpression. Mol Cell 21, 319–330.

Templeton TJ, Kaslow DC, Fidock DA (2000). Developmental arrest of the human malaria parasite *Plasmodium falciparum* within the mosquito midgut via CTRP gene disruption. Mol Microbiol 36, 1–9.

Triglia T, Healer J, Caruana SR, Hodder AN, Anders RF, Crabb BS, Cowman AF (2000). Apical membrane antigen 1 plays a central role in erythrocyte invasion by *Plasmodium* species. Mol Microbiol 38, 706–718.

Vahokoski J, Bhargav SP, Desfosses A, Andreadaki M, Kumpula E-P, Martinez SM, Ignatev A, Lepper S, Frischknecht F, Siden-Kiamos I, *et al*. (2014). Structural differences explain diverse functions of *Plasmodium* actins. PLoS Pathog 10, e1004091.

Vanderberg JP (1975). Development of infectivity by the *Plasmodium berghei* sporozoite. J Parasitol 60, 43–50.

Wesseling JG, de Ree JM, Ponnudurai T, Smits MA, Schoenmakers JG (1988). Nucleotide sequence and deduced amino acid sequence of a *Plasmodium falciparum* actin gene. Mol Biochem Parasitol 27, 313–320.

Wetzel DM, Hakansson S, Hu K, Roos D, Sibley LD (2003). Actin filament polymerization regulates gliding motility by apicomplexan parasites. Mol Biol Cell 14, 396–406.

Wong W, Webb AI, Olshina MA, Infusini G, Tan YH, Hanssen E, Catimel B, Suarez C, Condron M, Angrisano F, *et al*. (2014). A mechanism for actin filament severing by malaria parasite actin depolymerizing factor 1 via a low affinity binding interface. J Biol Chem 289, 4043–4054.

Zhang Q, Huang Y, Zhang Y, Fang X, Claes A, Duchateau M, Namane A, Lopez-Rubio J-J, Pan W, Scherf A (2011). A critical role of perinuclear filamentous actin in spatial repositioning and mutually exclusive expression of virulence genes in malaria parasites. Cell Host Microbe 10, 451–463.